Published online 30 August 2016 *Nucleic Acids Research, 2016, Vol. 44, No. 22* ***10539–10553***
doi: 10.1093/nar/gkw742

Chromatin recruitment of activated AMPK drives fasting response genes co-controlled by GR and PPARα

Dariusz Ratman[1,2], Viacheslav Mylka[1,2], Nadia Bougarne[1,2], Michal Pawlak[3,4,5,6], Sandrine Caron[3,4,5,6], Nathalie Hennuyer[3,4,5,6], Réjane Paumelle[3,4,5,6], Lode De Cauwer[1,2], Jonathan Thommis[1,2], Mark H. Rider[7], Claude Libert[8,9], Sam Lievens[2,10], Jan Tavernier[2,10], Bart Staels[3,4,5,6,11] and Karolien De Bosscher[1,2,*]

[1]Receptor Research Laboratories, Nuclear Receptor Lab, Medical Biotechnology Center, VIB, 9000 Ghent, Belgium, [2]Department of Biochemistry, Ghent University, 9000 Ghent, Belgium, [3]UNIV LILLE, 59000 Lille, France, [4]INSERM UMR 1011, 59000 Lille, France, [5]European Genomic Institute for Diabetes E.G.I.D., FR 3508, 59000 Lille, France, [6]Institut Pasteur de Lille, 59000 Lille, France, [7]de Duve Institute and Université catholique de Louvain, 1200 Brussels, Belgium, [8]Inflammation Research Center, VIB, 9052 Ghent, Belgium, [9]Department of Biomedical Molecular Biology, Ghent University, 9052 Ghent, Belgium, [10]Receptor Research Laboratories, Cytokine Receptor Lab, Medical Biotechnology Center, VIB, 9000 Ghent, Belgium and [11]CHU Lille, Department of Biology, 59000 Lille, France

Received July 28, 2015; Revised August 08, 2016; Accepted August 15, 2016

ABSTRACT

Adaptation to fasting involves both Glucocorticoid Receptor (GRα) and Peroxisome Proliferator-Activated Receptor α (PPARα) activation. Given both receptors can physically interact we investigated the possibility of a genome-wide cross-talk between activated GR and PPARα, using ChIP- and RNA-seq in primary hepatocytes. Our data reveal extensive chromatin co-localization of both factors with cooperative induction of genes controlling lipid/glucose metabolism. Key GR/PPAR co-controlled genes switched from transcriptional antagonism to cooperativity when moving from short to prolonged hepatocyte fasting, a phenomenon coinciding with gene promoter recruitment of phosphorylated AMP-activated protein kinase (AMPK) and blocked by its pharmacological inhibition. *In vitro* interaction studies support trimeric complex formation between GR, PPARα and phospho-AMPK. Long-term fasting in mice showed enhanced phosphorylation of liver AMPK and GRα Ser211. Phospho-AMPK chromatin recruitment at liver target genes, observed upon prolonged fasting in mice, is dampened by refeeding. Taken together, our results identify phospho-AMPK as a molecular switch able to cooperate with nuclear receptors at the chromatin level and reveal a novel adaptation mechanism to prolonged fasting.

INTRODUCTION

Peroxisome Proliferator-Activated Receptor α (PPARα) is a lipid sensing nuclear receptor activated by fatty acids (FA) and other lipid derivatives. High levels of PPARα coincide with the FA oxidative capacity of a tissue and are typically found in heart, liver and kidney (1). Additionally, its expression levels and activity significantly increase during fasting, which allows for the maintenance of physiological glucose levels and a switch toward FA oxidation and production of ketone bodies by the liver (2,3). The classic transactivation mechanism of PPARα involves hetero-dimerization with the Retinoid X Receptor and interaction with direct-repeat 1 type response elements. This mechanism is involved in the transcriptional control of a broad range of lipid metabolic genes (4). Besides its metabolic function, PPARα also exerts an anti-inflammatory activity by inhibiting NF-κB and AP-1 via a mechanism termed transrepression (5). Our recent data on the transrepression activity of PPARα link its

*To whom correspondence should be addressed. Tel: +32 9 264 9363; Fax: +32 9 264 9490; Email: karolien.debosscher@vib-ugent.be or karolien.debosscher@ugent.be
Present addresses:
Dariusz Ratman, Roche Global IT Solutions, Roche Polska Sp. z o.o., ul. Domaniewska 39B, 02-672 Warsaw, Poland.
Michal Pawlak, International Institute of Molecular and Cell Biology, Laboratory of Zebrafish Developmental Genomics, Warsaw, Poland.
Sam Lievens, Orionis Biosciences, Technologiepark 12B, 9052 Zwijnaarde, Belgium.

anti-inflammatory activity to the prevention of progression of chronic inflammation to fibrosis in the liver (6).

The glucocorticoid receptor (GR) is a nuclear receptor activated by steroidal stress hormones, glucocorticoids. Mechanistically, GR can signal as a homo-dimer recognizing palindromic glucocorticoid response elements (GREs) or via tethering of the GR monomer to other transcription factors, including AP-1 and NF-κB (7) or to GRE half sites (8,9). Ubiquitously expressed GR is predominantly studied for its potent anti-inflammatory action mechanisms (10). Nevertheless, endogenous glucocorticoids' (GCs) role extends beyond inflammation control given their important role in restoring energy homeostasis during nutrient deprivation. During prolonged fasting, GCs stimulate lipolysis and a flux of free FAs to the liver. This physiological response provides substrates for gluconeogenesis (11) and, together with a direct regulation of gluconeogenic gene expression by the GR, ensures sustained glucose levels during fasting. Cooperative molecular control mechanisms under a state of catabolic fasting are less well characterized, however.

AMP-activated protein kinase (AMPK) is a ubiquitously expressed kinase involved in cellular energy homeostasis. The canonical AMPK activation mechanism involves a response to increased cellular AMP levels, which may occur during states of nutrient deprivation, leading to increased AMPK α-subunit activation loop Thr172 phosphorylation. Activated AMPK switches off anabolic processes and promotes energy-generating catabolic pathways (12). Furthermore, pharmacological AMPK activation was shown to reverse GC-induced steatosis in non-fasted rat liver and to suppress GC-induced elevation of blood glucose and hepatic glycogen (13). Similarly to PPARα, AMPK activation stimulates the uptake and oxidation of FAs, although the mechanistic details of their relationship remain to be elucidated. In a previous study describing an additive anti-inflammatory effect of PPARα and GR, we demonstrated that both nuclear receptors can physically interact (14). Since both GR and PPARα are known to be active under fasting conditions and involved in the adaptation of an organism to nutrient deficiency, we therefore wondered if and how they could cross-talk in this context, and approached the question at a genome-wide level starting with a primary (murine) hepatocyte model. Via ChIP- and RNA-seq we mapped hepatic cistromes of GR and PPARα and coupled them to the transcriptional response observed upon single and combined agonist treatment. We show that both transcription factors mainly co-localize in the vicinity of lipid catabolism genes and cooperatively induce their expression when co-activated. By mimicking fed-to-fast and fast-to-fed transitions, we show a strong dependence of the cooperative response on hepatocyte nutritional status and demonstrate that under fasting conditions activated AMPK is directly recruited to promoters of the cooperatively induced genes in response to a combined GR/PPARα activation. AMPK activity is also required for the cooperative response as shown using a pharmacological AMPK inhibitor. GST-pull down assays demonstrate that recombinant activated AMPK, recombinant PPARα and *in vitro* translated GRα can physically associate, which might be indicative of a trimeric interaction model at key target gene promoters.

As a continued fasting coincides with an enhanced recruitment of phospho-AMPK at target gene promoters in liver—an effect that was partially inhibited following a short refeeding—we show that *in vitro* findings were also confirmed *in vivo*. Upon prolonged fasting, not only enhanced levels of phospho-AMPK were detected, but also enhanced levels of GR phosphorylated at Ser211. Finally, besides shedding light on the transcriptional coordination of glucose and FA metabolism by nuclear receptors, using metabolomics we show that a dual activation of GR and PPARα completely counteracts the accumulation of primary hepatocyte intracellular FAs observed upon treatment with GR-ligand alone, demonstrating an extension of the GR/PPARα cross-talk beyond gene pattern changes.

MATERIALS AND METHODS

Primary hepatocyte isolation

All experimental protocols were approved by the Lille Pasteur Institute ethical committee and carried out in agreement with European Union (EEC n°07430) and French ethical guidelines. Primary hepatocytes were isolated from 10–12 week old PPARα-WT or PPARα-KO C57BL/6 mice by collagenase perfusion (15). The procedure was modified by excluding insulin and Dex supplementation in the William's medium (Sigma, W1878). Additional culture details are provided in the Supplementary Materials and Methods.

ChIP

Each replicate was obtained by pooling cells from three animals. Stimulation was done for 1 h with: solvents (0.01% DMSO, 0.01% EtOH), 1 μM of Dexamethasone (Dex) (Sigma, D4902-25MG), 0.5 μM of GW7647 (GW) (Sigma, G6793-5MG) or a combination of Dex and GW. Single ligand treatments were additionally supplemented with the missing solvents. Proteins were cross-linked to DNA for 10 min using 1% formaldehyde and the cross-linking reaction was stopped by adding glycine to a final concentration of 0.125 mM. Cells were scraped in ice-cold phosphate buffered saline (PBS), washed 2x and snap frozen in liquid nitrogen before chromatin preparation and immunoprecipitation (IP). Detailed ChIP protocol is provided in the Supplementary Materials and Methods. For ChIP-seq, samples from 6 independent immunoprecipitations, obtained using 2 biological replicates were pooled, concentrated by drying and additionally sonicated (16) (20 cycles, 30 s on/30 s off, high intensity). Libraries were prepared using Illumina TruSeq Kit and subjected to a single-end 50 bp sequencing on the Illumina HiSeq 2000.

RNA-isolation

For RNA-seq and qPCR experiments primary hepatocyte cells were processed as described above. Stimulation was done for 19 h (RNA-seq and qPCR) or for 2, 4 and 6 h (time-kinetics qPCR). Each replicate was obtained by pooling cells from 3–4 mice and 3 independent replicates were used for RNA-seq and qPCR experiments. RNA was isolated with the RNeasy purification kit (Qiagen, cat. 74106) according to the user's manual. The RNA-seq library was

prepared using Illumina Tru-seq kit with poly-A selection and subjected to a single-end 50 bp sequencing on the Illumina GAII. For qPCR, cDNA was synthesized with a PrimeScript kit (Takara, cat. 6110B).

Metabolomics

For the metabolomics experiment, primary hepatocytes were isolated and stimulated as for ChIP experiments. Each sample was replicated independently six times. After 19 h of stimulation, cells were detached by 5 min trypsinization, resuspended in Dulbecco's modified Eagle's medium (DMEM) (Gibco, 41966-052) supplemented with 10% fetal bovine serum (FBS) and washed with PBS. Cell pellets were snap frozen in N_2 and processed further by Metabolon, Inc. (mView platform). Details of the sample processing are available upon request and additional information on the analysis is provided in the Supplementary Materials and Methods.

ChIP-seq analysis

Reads were mapped to the mm9 genome using Bowtie2 version 2.0.5. Peaks were called with MACS version 1.4.2 (17) (P-value $< 10^{-8}$) and filtered based on fold enrichment (>6x above input). Motif analysis was performed with meme-chip (18), homer (19) and FIMO (20). Distances between peaks and Transcription Start Sites' (TSS's) of differentially expressed genes were calculated with bedtools (21). More details are provided in the Supplementary Materials and Methods.

RNA-seq analysis

Reads were mapped to the mm9 genome using tophat (22) (version 2.0.7) supplied with ensembl annotation (parameters: –G, –no coverage search). Transcriptomes were assembled with cufflinks (23) (version 2.0.2, parameters: -q, -u, -b) and combined into a single assembly, including mm9 ensembl annotation with cuffmerge (parameters: -g, -s). The joint assembly was used as a reference for differential expression testing using cuffdiff (23) (parameters: -q, -N, -u, -b). Gene level differential expression analysis was performed with the aid of the R package 'cummeRbund' (24) by applying the following contrasts ($\alpha = 0.05$): NI (non-induced, i.e. solvent only) versus Dex, NI versus GW, NI versus DexGW, Dex versus DexGW and GW versus DexGW. Differentially expressed genes were combined into a single list (excluding non-protein coding genes), FPKM expression values were scaled across conditions (Z-score) and genes were re-ordered using a hierarchical clustering based on Euclidean distances. Data were partitioned into clusters by cutting the clustering tree at the height of 2.3, which resulted in 10 clusters. The result was visualized (Supplementary Figure S4) and expression patterns were examined to identify the main patterns of interaction between the ligands and guide significance testing for co-regulated genes. Two smallest clusters with 1 and 3 genes, respectively, where omitted from the visualization and peak/gene ontology (GO) enrichment analysis. The following filter was used to extract cooperatively induced genes: up-regulation by DexGW as compared to NI and significantly higher expression in DexGW as compared to Dex and GW alone. GO-analysis of gene clusters was performed using 'goseq' R-package (25). All enrichment p-values in GO analysis were corrected for multiple testing using the Benjamini–Hochberg method.

Accession numbers

ChIP-seq and RNA-seq data have been uploaded to the NCBI-SRA repository and are available under SRP058743 accession.

qPCR and ChIP-qPCR

qPCR's were performed using Light Cycler 480 SYBR Green I Master Mix (Roche, cat. 04887352001) (primer list provided in the Supplementary Materials and Methods). qPCR data were normalized and quantified relative to the two most stable reference genes with qBase (26) and expressed relative to the control (NI) condition. Statistical analysis was performed using R (R Core Team (2014) R: A Language and Environment for Statistical Computing) and GraphPad Prism (see details in figure legends).

MAPPIT

MAPPIT was performed as described earlier (27), with its principle depicted in Figure 6C. Briefly, Hek293T cells were seeded at the density of 10 000 cells/well on a 96 well plate in DMEM (Gibco, 41966-052) supplemented with 10% FBS. Next day 25 ng of bait, 50 ng of prey and 5 ng of the STAT3-dependent pXP2d2-rPAPI-luciferase reporter vector were transfected using a standard calcium phosphate transfection method. After 24 h, the reporter was stimulated with leptin (100 ng/ml) and reporter activity was measured 24 h after leptin stimulation using the Luciferase Assay System kit (Promega) on an Envision luminescence plate reader (Perkin–Elmer). Signals for each interaction are presented as fold induction of the luciferase signal of leptin-stimulated versus unstimulated samples. The fold induction is a measure of the interaction strength.

The pXP2d2-rPAPI-luciferase reporter vector (28), the plasmids encoding the full size GR bait (pCLG-GR; (29) and the irrelevant bait containing a fusion with *E. coli* DHFR (pCLG-eDHFR; (30)) and the empty control prey plasmid encoding unfused gp130 (pMG1) have been described previously (27). The PRKAG2 and PRKAG3 prey plasmids (pMG1-PRKAG2 and pMG1-PRKAG3, respectively) were generated by Gateway (Thermo Fisher Scientific) recombinatorial cloning of the full size PRKAG2 and PRKAG3 entry clones from the human ORFeome version 8.1 collection (31) into the pMG1 vector as described (27). The PPARα bait plasmid (pCLG-PPARα) was generated by substituting the GR encoding sequence of the pCLG-GR vector with the full size coding sequence of PPARα.

GST-pull down

Anti-GST beads Glutathione Sepharose 4B beads (GE Healthcare Life Sciences cat. 17-0756-05) were incubated

with GST-PPARα or GST-5HT7 (negative control) in NETN-buffer (20 mM Tris-HCl pH8, 100 mM NaCl, 6 mM MgCl2, 1 mM EDTA, 0.5% NP40, 1% DTT, Complete Protease Inhibitor Cocktail (Roche cat. 11836145001) and protein phosphatase inhibitors (1 mM NaF and 1 mM $NaVO_3$)). Beads were first blocked with NETN-buffer + 2% nonfat milk powder for 1 h. Next, GST-protein binding beads were washed 3x in NETN-buffer and re-suspended in 280 μl modified NETN-buffer (20 mM Tris-HCl pH8, 8% glycerol, 300 mM NaCl, 6 mM MgCl2, 1 mM EDTA, 0.05% NP40, 1% DTT, Complete Protease Inhibitor Cocktail (Roche cat. 11836145001) and protein phosphatase inhibitors (1 mM NaF and 1 mM $NaVO_3$)). Activated and His-tagged AMPK complex α1β2γ1 (2.6 μg/sample) together with *in vitro* transcribed and translated proteins (TnT Quick Coupled Transcription/Translation System, Promega, cat. L1170) were added to bead solution at a volume as indicated in the Figure, together with 0.5 μM of GW7647 and 1 μM of Dex. Binding reaction was carried out at 4°C with rotation overnight. Following 3 wash steps with modified NETN-buffer, proteins were eluted with Laemmli buffer, boiled for 3 min and loaded on the gel for Western Blot analysis. Active AMPK was detected with anti-phospho-Thr172 AMPKα1/2 (Santa-Cruz, sc-33524), GR with anti-GR (H-300, Santa Cruz, sc-8992) and GST-PPARα and GST-5HT7 ctrl (kind gift of Dr K. Van Craenenbroeck, UGent) with anti-GST (Abcam, cat ab9085). Recombinant bacterially expressed AMPK ($\alpha_1\beta_1\gamma_1$) was activated with recombinant bacterially expressed LKB1-MO25-STRAD complex (Bultot *et al.* 2012), both kindly provided by Dietbert Neumann (Institute of Cell Biology, ETH Zurich, CH).

In vivo analysis

C57BL/6J male mice of 8 weeks old were obtained from Charles River. The specific treatment set-up has been specified in the legend of Figure 7. In panel A, 10 male mice underwent a 16 h starvation regimen. Groups were subsequently split in two, with 5 mice allowed a refeeding ('fast-refed') whilst the other 5 mice stayed fasting ('fast-fast'). Thirty minutes later, mice were sacrificed; both sera and livers were collected for analysis. In panel C, 5 mice/group were fasted for either 3 h or 16 h, after which either placebo or a combination of water-soluble Dex (2 mg/kg) and GW (2 mg/kg) was given i.p. Four hours later, mice were sacrificed and the liver was analyzed for mRNA expression via qPCR analysis. Experiments were approved by the animal ethical committee of the faculty of medicine at the University of Ghent (code dossier 14/84).

RESULTS

Shared binding sites of GR and PPARα concur with an enrichment of GRE and PPRE motifs

For an unbiased insight into the genomic cross-talk between GR and PPARα, we performed a ChIP-seq experiment using primary murine hepatocytes treated for 1 h with solvents (non-induced – NI), dexamethasone (Dex), GW7647 (GW) and a combination of Dex and GW. In total, we detected 15 619 and 3541 genomic binding sites for GR and

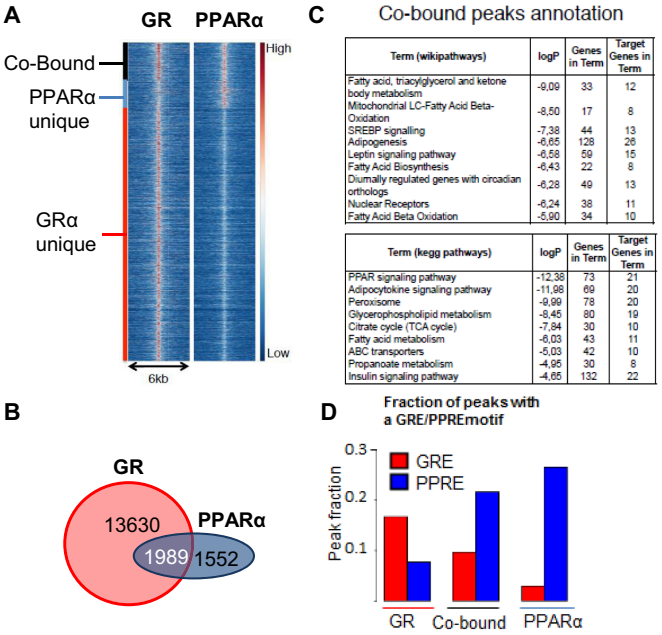

Figure 1. Glucocorticoid receptor (GR) and peroxisome proliferator-activated receptor α (PPARα) binding sites (primary murine hepatocytes ChIP-seq) co-occupancy, motif enrichment and GO annotation. (**A**) The heatmap shows normalized tag densities (represented by the color scale) for GR and PPARα on unique and co-bound peaks upon combined ligand treatment. (**B**) Venn diagram representation of binding sites overlap. (**C**) The functional annotation of co-bound peaks using GO terms associated with the nearest genes. (**D**) Fraction of unique and co-bound peaks with *de novo* GRE or PPRE motifs as identified by MEME-ChIP/FIMO (P-value $< 10^{-4}$) (see also Supplementary Figure S1).

PPARα, respectively. No major rearrangement of the binding sites was observed when comparing single and combined ligand stimulations (Supplementary Figure S1A and B), hence we intersected complete sets of GR and PPARα peaks to test the extent of the peak overlap. Using 200 bp as a maximum summit-to-summit distance between peaks to consider them as overlapping, 1989 peaks were identified passing this threshold. This number represents a significant fraction of all PPARα peaks (56%), and—given the higher total number of GR binding sites—a relatively smaller subset of GR peaks (13%) (Figure 1A and B). Analysis of pathway enrichment terms among genes in the vicinity of overlapping peaks showed a consistent enrichment of terms related to lipid metabolism, suggesting a possible preferential co-regulation of those genes by GR and PPARα (Figure 1C). To gain mechanistic insight, we investigated which motifs are enriched among overlapping peaks as compared to peaks uniquely bound by each receptor (Supplementary Figure S1C–F). Compared to uniquely bound GR peaks, overlapping ones were mainly enriched for PPRE and PPRE-like motifs (Supplementary Figure S1F). Conversely, when uniquely bound PPARα peaks were used as a background, co-bound peaks were predominantly enriched for GRE and GRE-like motifs, such as PRE and AR/GR-half-sites, together with C/EBP and HNF6 (Supplementary Figure S1E). This result was further confirmed by a targeted motif scan using *de novo* generated GRE and

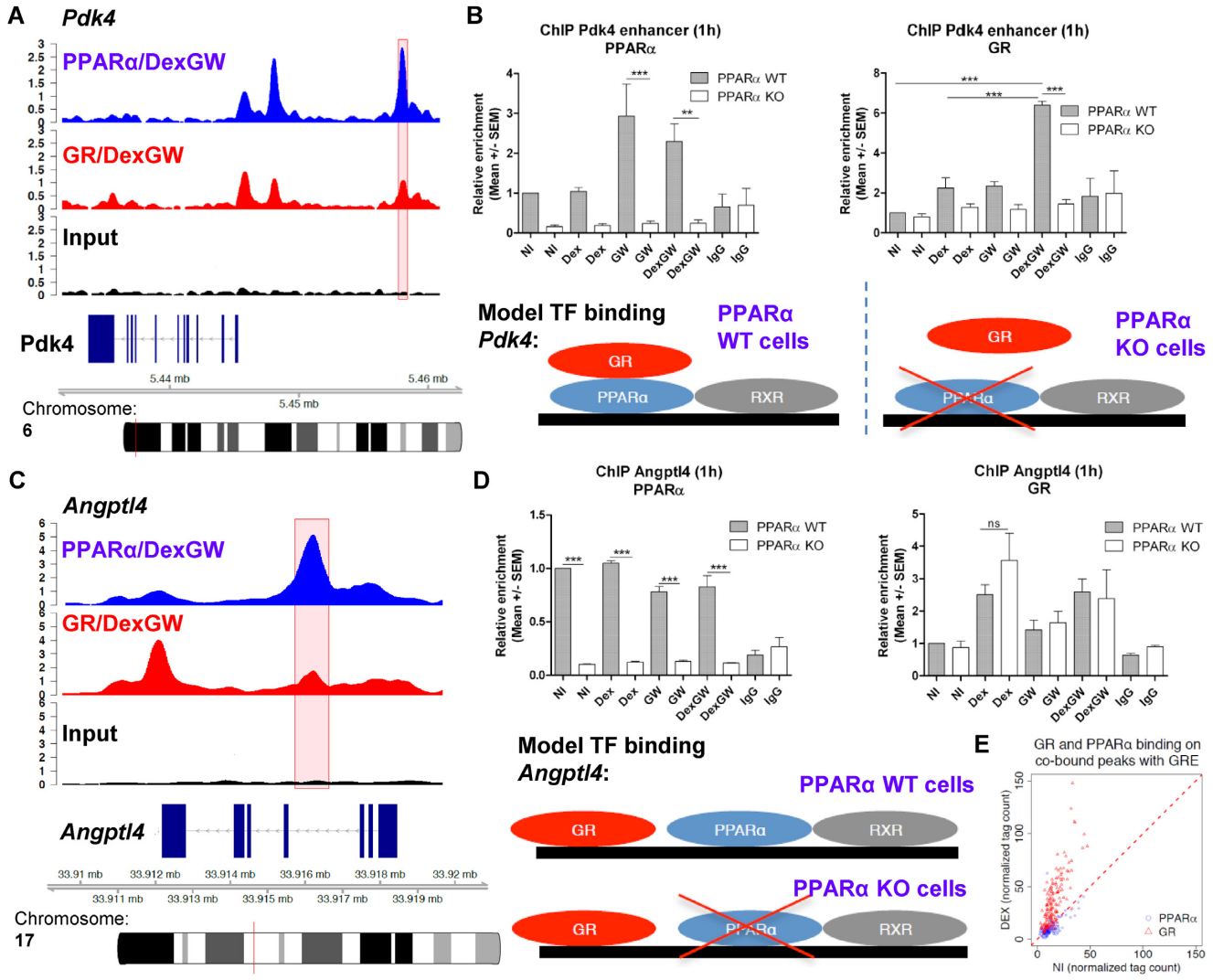

Figure 2. Binding of GR and PPARα to co-bound peaks with PPRE motifs in primary hepatocytes from PPARα-WT and -KO mice. (**A**) ChIP-seq profiles of GR and PPARα at the *Pdk4* upstream enhancer. (**B**) ChIP-qPCR on the *Pdk4* enhancer and a model illustrating co-occupancy via a tethering mechanism. (**C**) ChIP-seq profiles of GR and PPARα within the *Angptl4* intron. (**D**) ChIP-qPCR on the *Angptl4* intron and a model illustrating co-occupancy via independent binding. The pink rectangles on the ChIP-seq tracks (A and C) mark peaks, which were tested via ChIP-qPCR and bar plots show enrichment relative to non-induced (WT) sample. Statistical analysis (one-way-ANOVA with a Tukey post-hoc test, n = 3) is shown for selected comparisons (** and *** denote *P*-values < 0.01 and < 0.001, respectively). (**E**) The scatter plot shows ChIP-seq tag counts for GR and PPARα co-bound sites with GRE in NI and Dex conditions. NI, non-induced (solvent only), Dex, Dexamethasone.

PPRE motifs. Thus, GR and PPARα could interact with close co-occurring motifs within shared binding sites. A higher frequency of PPREs as compared to GREs in overlapping peaks (Figure 1D) also suggested a possibility for indirect GR recruitment via tethering to PPARα.

Co-recruitment of GR to shared PPRE-containing binding regions shows site-specific dependency on PPARα

In order to test whether GR recruitment to select co-bound regions with PPRE motifs is dependent on PPARα, we compared primary hepatocytes from PPARα-WT and -KO mice (32). When examining PPRE-containing co-bound regions upstream of *Pdk4* (Figure 2A) and in the gene body of *Angtpl4* (Figure 2C) via ChIP analysis, we found that for both model genes the PPARα signal was lost in PPARα-KO hepatocytes, as expected (Figure 2B and D, left panels). This was also confirmed for six additional, PPRE-containing co-bound regions tested (Supplementary Figure S2). Interestingly, the absence of PPARα also influenced GR recruitment to a subset of the shared binding sites tested. The intronic site within *Angptl4* and the *Pdk4* enhancer represent two extreme cases where GR-binding is either completely lost (Figure 2B, right panel) or unaffected (Figure 2D, right panel) in PPARα-KO cells, respectively. The GR signal was also significantly reduced in the presence of both ligands when comparing WT with PPARα-KO at sites near *Agpat3* and *Plin5*. Similar, trends were observed for peaks near *Eci2*, *Acadl1* and *Cbfa2t3* but effects did not meet a significance threshold (Supplementary Figure S2).

To extend the analysis and interrogate whether PPARα activation can influence GRE-bound GR, we made use of the fact that DNA binding of GR, in contrast to PPARα, is strongly ligand dependent. Therefore, one would expect that in the case of tethering, PPARα occupancy in co-bound regions harboring a GRE should increase following Dex stimulation. Our analysis shows that GR occupancy at these sites indeed clearly increases in the presence of Dex. However, PPARα occupancy remains largely unaffected (Figure 2E), arguing against a tethering of PPARα to GRE-bound GR. As an additional control, by using EMSA analysis we excluded that independent binding could alternatively be explained by direct recruitment of GR to PPRE motifs and vice versa – PPARα to GRE (Supplementary Figure S3). In summary, we conclude that while the recruitment of GR via either tethering to PPARα or else assisted by a pioneering role for PPARα is possible (as shown for *Pdk4*, *Plin5* and *Agpat3*), their frequent close co-localization can also represent independent binding events (as shown for *Angptl4* and *Dpep2*) – facilitated either directly via co-occurring PPRE and GRE motifs or else via an interaction with other transcription factors or non-canonical/degenerate motifs present in co-bound regions.

Co-activation of GR and PPARα triggers cooperative activation of lipid metabolic pathways and counteracts Dex-induced hepatic FA accumulation

Frequent co-localization of GR and PPARα on the chromatin prompted us to further investigate the transcriptional cross-talk. To this end we performed RNA-seq analysis in primary murine hepatocytes upon single and combined ligand stimulation. Differentially expressed genes were identified for a set of pairwise contrasts (NI versus Dex, NI versus GW, NI versus DexGW, GW versus DexGW and Dex versus DexGW) (Supplementary Figure S4), combined into a single list and next fed into a hierarchical clustering algorithm to identify predominant expression patterns across treatments (Supplementary Figure S5). With this approach we could partition the data into eight main clusters (Supplementary Figure S5), which were further analyzed for enrichment of GO terms (Supplementary Table S1) and presence of nearby GR and PPARα binding sites (Supplementary Figure S5). For all gene clusters, nearby GR peaks were more common than PPARα peaks, which is not surprising given their larger total number and more genes differentially expressed in response to Dex as compared to GW (Supplementary Figure S4). However, two clusters (Supplementary Figure S5 clusters 1 and 2) stood out as (i) cooperatively activated, (ii) highly enriched with peaks for both receptors and (iii) enriched for similar GO terms related to lipid metabolism (Supplementary Table S1). To narrow this list down, we retrieved differentially expressed genes for which expression upon combined stimulation was significantly higher than for each ligand alone (False Discovery Rate = 5%), which yielded 93 high confidence, cooperatively induced genes (Figure 3A). Repeating the functional annotation on this smaller gene set confirmed strong enrichment of terms related to lipid metabolism (Figure 3B), while peak enrichment analysis established that these are potentially direct targets, i.e. we could detect binding sites for GR and PPARα within 20 kb from TSSs for close to 80% of those genes (Figure 3C). Example genes in this group encode proteins involved in the release of FA from adipose tissue (Angptl4) (33), FA transport (Fabp4, Cpt1a, Cpt2) (34–36), FA activation (Acot1, Acot2) (37,38), triglyceride hydrolysis (Pnpla2/Atgl) (39) and ketone body synthesis (Hmgcs2) (40) as well as enzymes involved in FA β-oxidation such as Acox1, Hadha, Hadhb, Ehhadh, Eci2, Acadl and Acadvl. So far, the overall data indicate that genomic co-localization of GR and PPARα underlies a cooperative transcriptional response that shifts the primary hepatocyte metabolism toward increased lipid utilization.

To find out whether and how the gene-regulatory events upon combined ligand treatment translated into changes at the FA metabolite levels, we performed a metabolomics experiment using primary hepatocytes stimulated with Dex, GW and their combination using the same conditions and stimulation time (19 h) as in the RNA-seq experiment. The pattern of ligand response among significantly perturbed FAs was uniform and with the exception of myristate, Dex treatment increased the quantity of all other FAs. Strikingly, this increase was almost completely reversed upon combined stimulation with Dex and GW (Figure 4A and B). Hence, the combination of Dex and GW modulates the activity of the key controlling genes/enzymes in such a way that the FA content of the hepatocyte is normalized back to control levels.

Transcriptional antagonism can switch to cooperativity when hepatocyte cells move from fed to fasting states in culture

The cooperative response and its dependency on the presence of PPARα (19 h stimulation) were confirmed for a panel of selected target genes (Figure 5A). To find out whether all of the co-controlled target genes responded to ligand with a similar kinetics, we recapitulated the experiment including shorter incubation times (2 h, 4 h, 6 h). To our surprise, for a subset of re-tested genes the direction of this regulation showed an intriguing dependency on the stimulation time (Figure 5B). Specifically, upon a short stimulation (2 h) we observed an antagonistic effect of adding Dex with respect to the GW-only induction for *Pdk4*, *Ehhadh* and *Angptl4* – genes cooperatively activated upon longer treatment (Figure 5B, black versus light grey bars, compare DexGW versus GW, marked with red versus blue arrows for *Pdk4* and *Eci2* as opposite examples). In line herewith, for the same genes, the antagonism is also observed assessing pPol2-Ser2 enrichment as a marker for transcriptional activity, upon 1 h stimulation (Supplementary Figure S6). This initial antagonism was completely lost when including an additional starvation step to lose potential confounding endogenous factors, by incubating isolated hepatocytes in serum-free William's medium for an extra 24 h prior to stimulation. Interestingly, the overall magnitude of the cooperative response was also enhanced in this setting (Figure 5C).

Given those results and the fact that mice used for hepatocyte isolation were not fasted, we hypothesized that the antagonistic effect at shorter ligand induction times may result from a prior exposure of cells to high glucose and insulin, concomitant with a fed state. To test how a change in

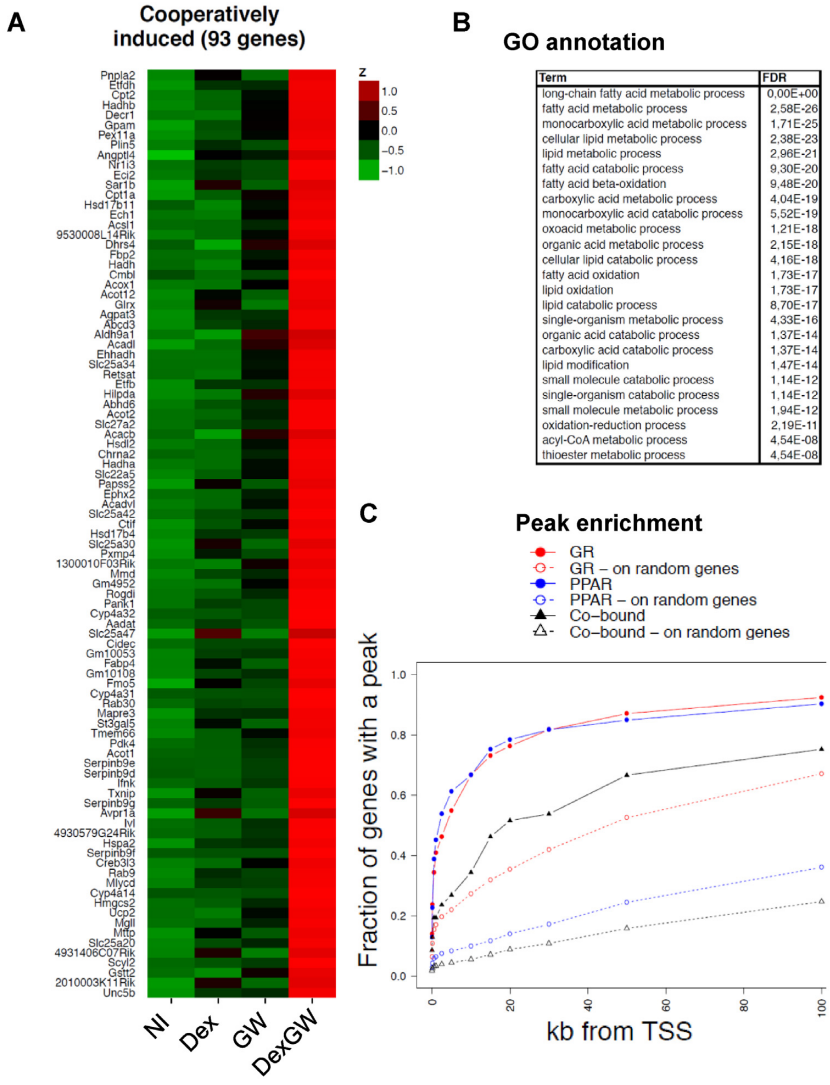

Term	FDR
long-chain fatty acid metabolic process	0,00E+00
fatty acid metabolic process	2,58E-26
monocarboxylic acid metabolic process	1,71E-25
cellular lipid metabolic process	2,38E-23
lipid metabolic process	2,96E-21
fatty acid catabolic process	9,30E-20
fatty acid beta-oxidation	9,48E-20
carboxylic acid metabolic process	4,04E-19
monocarboxylic acid catabolic process	5,52E-19
oxoacid metabolic process	1,21E-18
organic acid metabolic process	2,15E-18
cellular lipid catabolic process	4,16E-18
fatty acid oxidation	1,73E-17
lipid oxidation	1,73E-17
lipid catabolic process	8,70E-17
single-organism metabolic process	4,33E-16
organic acid catabolic process	1,37E-14
carboxylic acid catabolic process	1,37E-14
lipid modification	1,47E-14
small molecule catabolic process	1,14E-12
single-organism catabolic process	1,14E-12
small molecule metabolic process	1,94E-12
oxidation-reduction process	2,19E-11
acyl-CoA metabolic process	4,54E-08
thioester metabolic process	4,54E-08

Figure 3. Gene expression profiling in primary hepatocytes stimulated with GR- and PPARα-agonists. (**A**) Heatmap shows the relative expression of the cooperatively induced genes. Color scale represents fragments per kilobase per million values scaled across treatments (z-score). (**B**) Enrichment of the GO-terms for the cooperatively induced genes, 20 most significant terms are shown in the table (see also Supplementary Figures S4 and S5). (**C**) Enrichment of ChIP-seq peaks near Transcription Start Sites (TSS) of the co-regulated genes – the fraction of genes with a GR, PPARα or co-bound peak at a given distance from the TSS as compared to a random set of genes is shown. NI, non-induced (solvent only).

nutritional conditions affects the response to Dex and GW, we set up a model to mimic fed-to-fast and fast-to-fed transitions in primary hepatocyte cultures. We used a high glucose (11 mM) medium supplemented with insulin (100 nM) as a surrogate for the fed state and a low glucose (1 mM) medium supplemented with pyruvate (1 mM), glutamine (2 mM) and forskolin (10 μM) to simulate a fasting state (see Materials and Methods for details). Isolated cells were first pre-incubated in serum-free William's medium for 24 h (as in Figure 5C) to eliminate the influence of endogenous factors. Cells were next put for 3 h in either 'fed' or 'fast' medium and stimulated with ligands after alternating the media from 'fed' to 'fast' or 'fast' to 'fed'. We could clearly reproduce the regulation-switch in the fed-to-fast condition for *Pdk4* as one of the prototypical genes for which GW-mediated induction was strongly antagonized by Dex after 2 h and cooperatively induced after 6 h (Supplementary Figure S7). However, prolonged hepatocyte culturing resulted in a diminished response to GW in case of *Angptl4* and *Ehhadh*, which prevented us from recapitulating early antagonism for those two genes. Nevertheless, a clear suppression of the cooperative response in fast-to-fed as compared to the fed-to-fast condition was apparent, suggesting sensitivity of the response to a nutritional context. Among the tested genes, this suppression was especially clear for *Cpt1a* and *Hmgcs2*, which are rate-limiting enzymes for FA oxidation and ketogenesis, respectively (Supplementary Figure S7A). In line with our previous findings, initial antagonism was not observed for *Eci2*, *Plin5* and *Agpat3*, confirming that this type of regulation is restricted to a subset of lipid metabolism-controlling genes. For all of the genes, however, a pronounced cooperativity is consistently observed upon combining GW and Dex in a fasting state. Because of the time-dependency of the cooperative effect, we wondered

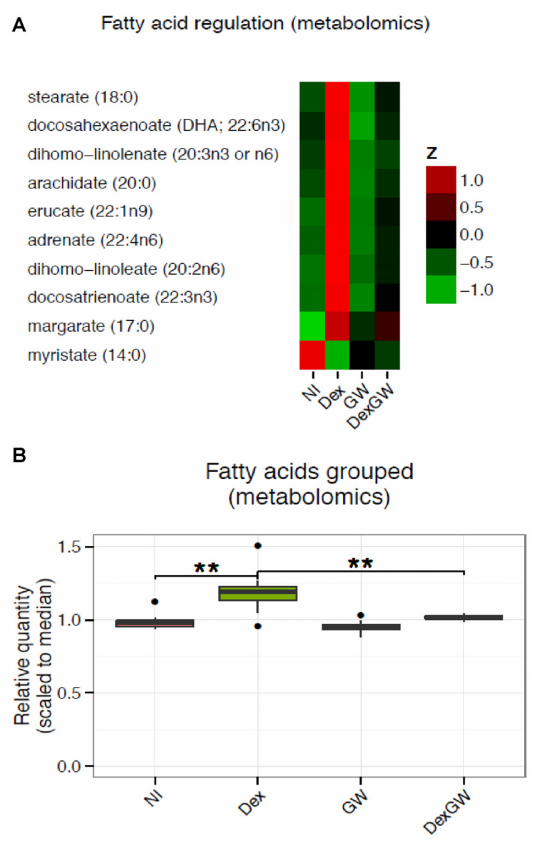

Figure 4. The effect of Dex and GW on the hepatic fatty acid content (metabolomics). (**A**) Heatmap showing regulation of significantly perturbed fatty acids in the metabolomics experiment. (**B**) Boxplot comparing the global ligand effects on all significantly perturbed fatty acids (black dots indicate outliers). The '**' denotes a *P*-value < 0.01 as assessed using Welch's t-test with a Bonferroni correction. NI, non-induced (solvent only).

whether novel protein production might facilitate and precede the fasting response. Indeed, inclusion of the protein synthesis inhibitor cycloheximide in the fed-to-fast set-up eradicated cooperative gene inductions at 6 h, of two exemplary target genes *Eci2* and *Pdk4* (Supplementary Figure S7B).

Transcriptional cooperativity of GR and PPARα co-controlled lipid metabolism genes coincides with a strong recruitment of phosphorylated AMPK to the promoter complex

Given the suppression of cooperativity upon entry into the fed state, we speculated that the nutrient sensing kinase AMPK, which is known to be inhibited by high insulin and glucose levels (41,42) could be involved in the cooperative cross-talk between GR and PPARα. In support, we observed a complete suppression of the response to Dex and GW and no cooperativity in the fed-to-fast condition when cells were co-treated with the pharmacological AMPK inhibitor dorsomorphin (Figure 6A), also known as Compound C. As a control, we verified that this pharmacological compound did not generally inhibit gene transcription by comparing total mRNA levels and by assessing mRNA levels of *GAPDH*, *SCD1* and *Hsp70* (data not shown). To test whether AMPK is directly involved in the GR and PPARα-mediated transcriptional regulation we performed a ChIP-qPCR experiment in the fed-to-fast condition upon 1 and 5 h stimulation with Dex and GW. In parallel with the promoter recruitment of phospho-Thr172 AMPK (pAMPK) we monitored pPol2-Ser2 as a marker of a transcriptional activity. Shortly after the entry into the fast state (1 h stimulation) we did not detect any major changes in pAMPK recruitment and pPol2-Ser2 showed only a small increase for *Eci2*, while for *Pdk4* there was a decrease upon co-stimulation as compared to GW alone, which is in line with the previously observed strong early antagonistic response for this gene. However, pAMPK was recruited after 5 h in a cooperative manner upon co-stimulation and its appearance also coincided with a cooperative increase in pPol2-Ser2 signal (Figure 6B). Using the mammalian two-hybrid assay, termed MAPPIT (27,43) (Figure 6C) we also identified a statistically significant interaction between two regulatory subunits of AMPK (PRKAG2/AMPK-γ2 and PRKAG3/AMPK-γ3) and full length PPARα but not full length GR (Figure 6C). GST-pull down analysis using GST-PPARα combined with a recombinant LKB1-activated pAMPK (α1β2γ1) heterotrimeric complex (44), and *in vitro* transcribed and translated GRα in reticulocyte lysates shows that, at least *in vitro*, a signal for GRα can be detected when PPARα is pulled down along with recombinant active pAMPK (Figure 6D and Supplementary Figure S8) suggesting a physical complex harboring these three proteins is possible. The interaction data suggest that a contact interface involving PPARα and the γ-subunits of AMPK may support promoter recruitment of the pAMPK complex, in a constellation that may additionally accommodate GRα. Overall, the data add up to a model whereby recruitment of pAMPK to GR and PPARα co-controlled genes in response to a combined agonist treatment is required for their full transcriptional activity.

Catabolic fasting in mice correlates with an increased recruitment of phosphorylated AMPK at the *Pdk4* enhancer

To validate the *in vitro* observations *in vivo*, mice were subject to a prolonged fasting of 16 h and either allowed to stay on this regimen ('fast-fast') or allowed to refeed ('fast-refed') for 30 min before sacrifice. Glucose levels in the fasting states ranged between 100–150 mg/dl whereas those in the refed state ranged between 150–200 mg/dl, indicating a normal response to refeeding (data not shown). Using ChIP-qPCR, we confirmed that pAMPK is robustly recruited to the *Pdk4* enhancer under the fast-fast condition and that this enrichment undergoes suppression in case of a short refeeding (Figure 7A). Similar findings were made for *Ehhadh* (data not shown). As a control and as expected, we observed a global decrease in AMPK phosphorylation upon refeeding without a change in the total AMPK expression levels (Figure 7B, left panel). Together, these data confirm that the chromatin recruitment of pAMPK in liver is responsive to fast/refeeding signals. In line with a role for GR Ser211 phosphorylation when GR is transcriptionally active (45), overall pSer211 GR levels were higher in the 'fast-fast' state as compared to the 'fast-refed' state (Figure 7B, right panel). Finally, to investigate whether the observed

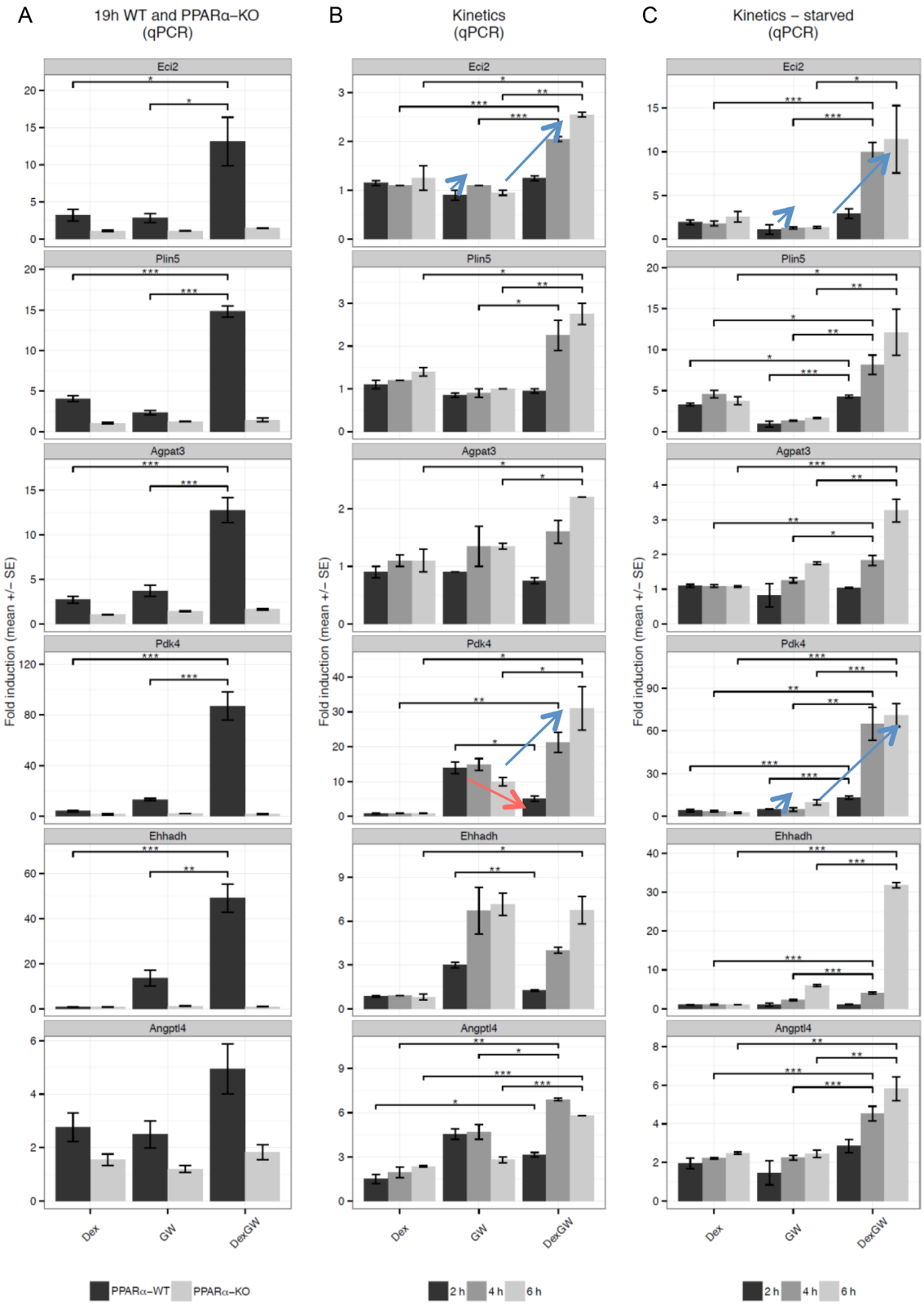

Figure 5. qPCR analysis of the selected cooperatively induced genes (primary murine hepatocytes). (**A**) Comparison of WT and PPARα-KO cells upon stimulation in Wiliams medium for 19 h. Ligands were introduced 2h after isolation (as in the RNA-seq). (B and C) Time kinetics of the response; (**B**) ligands (1 μM Dex, 0.5 μM GW) were introduced 2 h after hepatocyte isolation or (**C**) after 24 h serum-starvation. Fold induction upon combined ligand stimulation was compared with single ligand treatments using one-way ANOVA and Dunnett's test (*, ** and *** denote *P*-values < 0.05, 0.01 and 0.001, respectively, n = 3 (panels A and C) or 2 (panel B)) (see also Supplementary Figure S5).

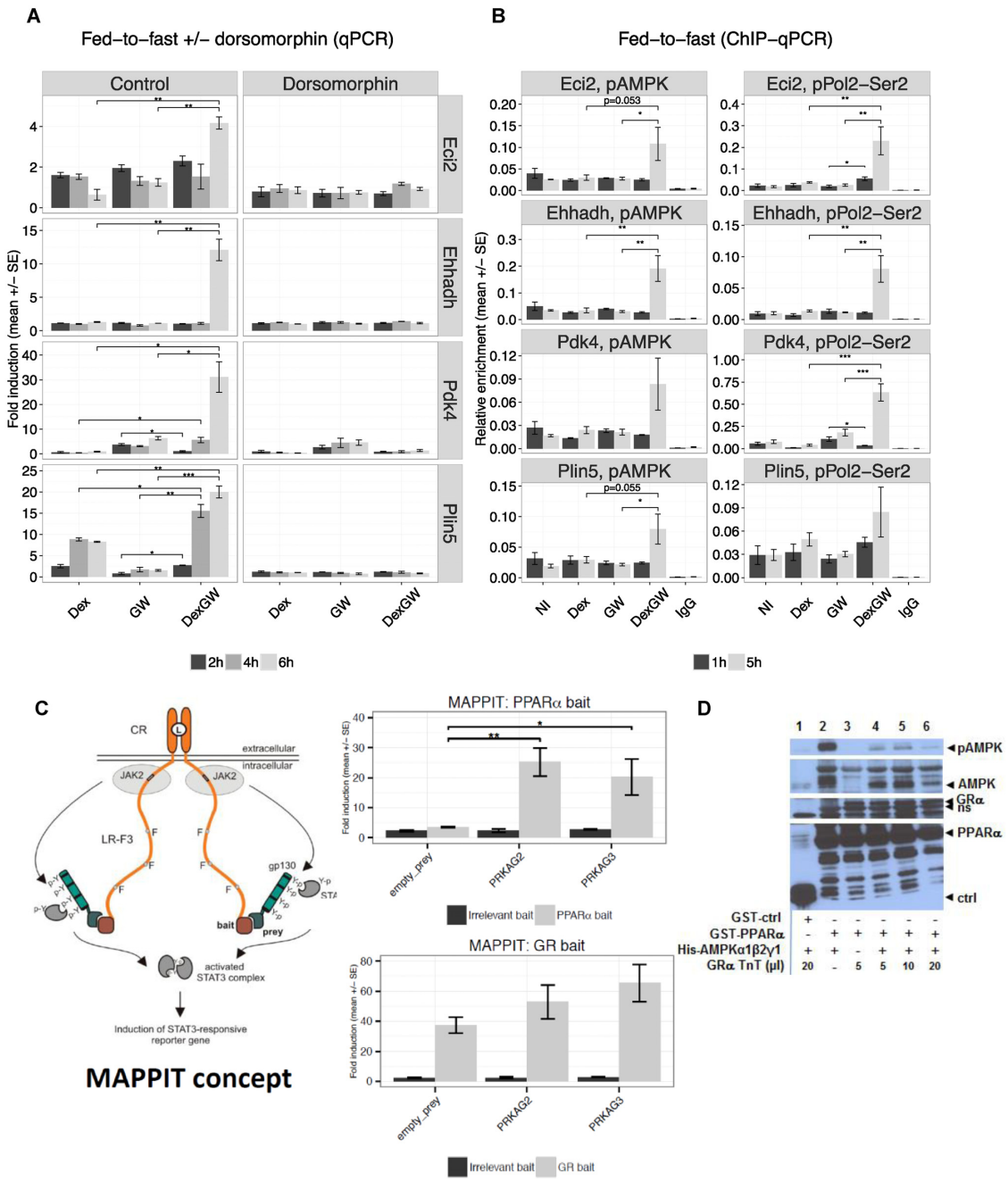

Figure 6. The involvement of AMPK in the response to GR-/PPARα-ligands. Hepatocytes were serum-starved for 24 h after isolation, incubated for 3 h in the medium mimicking fed state and stimulated with ligands (1 μM Dex, 0.5 μM GW) after switching to the fasting medium for the indicated time points. (**A**) The effect of ligands on gene expression (qPCR) in the presence/absence of dorsomorphin (10 μM). (**B**) Promoter recruitment of phospho-Thr172 AMPK and phospho-Ser2 Pol2 in response to ligand treatment (ChIP-qPCR). Fold induction (qPCR) or relative enrichment (ChIP-qPCR) upon combined stimulation was compared with single ligand treatments using one-way ANOVA and Dunnett's test (*, ** and *** denote *P*-values < 0.05, 0.01 and 0.001, respectively, n = 2 (panel A) or 3 (panel B)). (**C**) Left panel. The scheme illustrates the concept of the MAPPIT technology (reprinted with permission from (27). Copyright 2009 American Chemical Society). In short, full length bait protein is fused to a signaling-deficient cytokine receptor (Y to F mutations), in this case the leptine receptor and the prey protein is fused to gp130 domain containing JAK2 phosphorylation sites. Upon bait-prey interaction the gp130 domain is phosphorylated by JAK2 in response to cytokine receptor stimulation, allowing the recruitment of STAT3 to phosphorylated gp130 sites and subsequent phosphorylation and activation of STAT3. Activated STAT3 translocates to the nucleus and induces the expression of the STAT3-responsive reporter. The induction of the STAT3-reporter in response to a cytokine is used as a proxy of the bait-prey interaction strength (for detailed explanation see (27)). Right panel. Interaction between full length PPARα/GR-bait, activated by their respective ligands Dex (1 μM) and GW (0.5 μM) and full length AMPK subunits. * and ** indicate *P*-values < 0.05 and < 0.01 as assessed with the Welch's t-test and Holm *P*-value correction, n = 3. (**D**) GST-pull down experiment demonstrating interaction between GST-PPARα with *in vitro* transcribed/translated GR and recombinant activated AMPK complex (α1β2γ1) in the presence of Dex and GW7647. Of note, the strong signal for pAMPK associating with GST-PPARα in lane 2 is caused by the fact that this positive control set-up was performed in the absence of rabbit reticulocyte lysate in the binding mix. ns: non-specific band. GST-ctrl: GST fused to a 5HT7 serotonin receptor domain was used as a negative control.

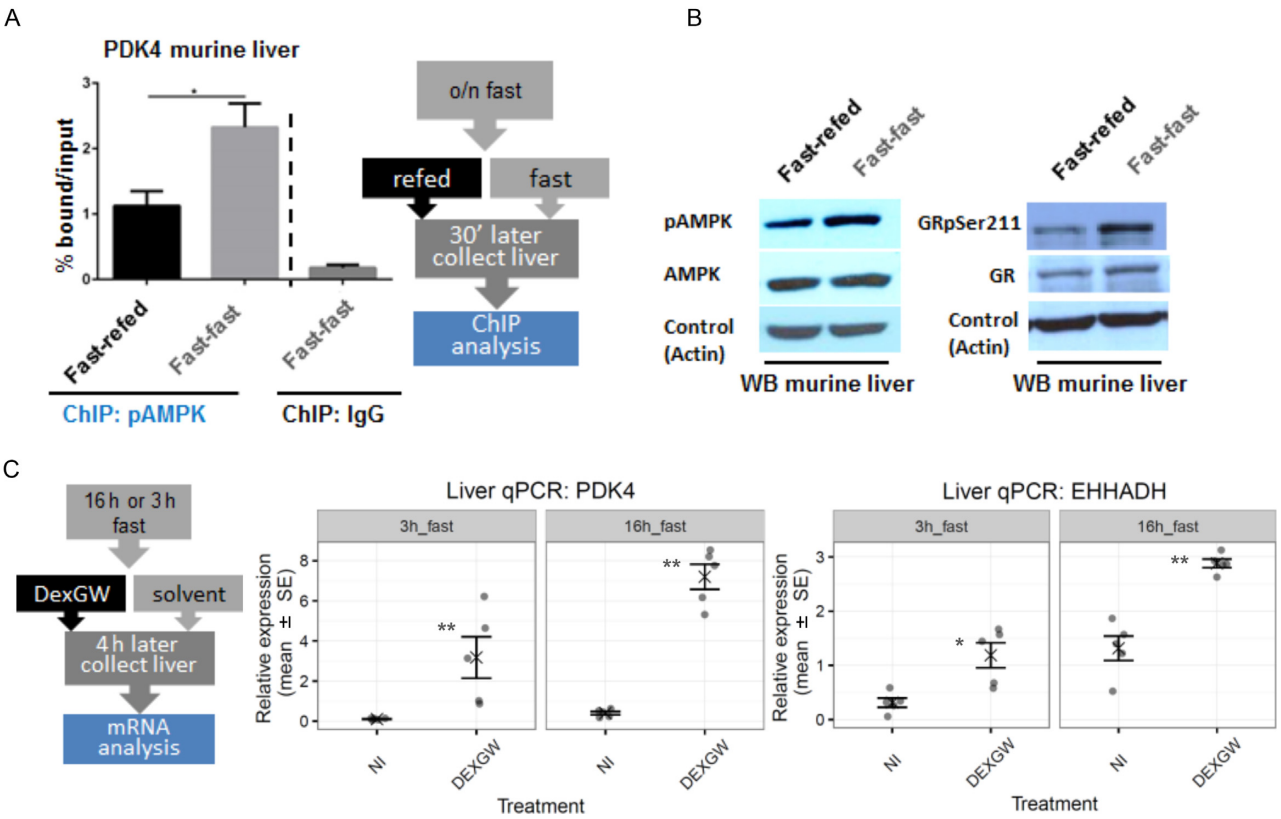

Figure 7. Catabolic fasting in mice correlates with an increased recruitment of phosphorylated AMPK at the *Pdk4* enhancer (**A**) Mice (5 mice/group) were subject to overnight fasting, and subsequently allowed to a refeeding step for 30 min or kept at a fasting state. After the sacrifice, livers were collected, snap-frozen and used for ChIP-qPCR or for WB. ChIP-qPCR with anti-pAMPK antibody or IgG: The enrichment data are presented relative to input chromatin and represents the mean value from 5 mice ± SE. The statistical significance was assessed using a two-tailed t-test and '*' denotes *P*-value < 0.05. (**B**) Western analysis result of one group of the experiment in (A) probed for liver AMPK and pAMPK (left panel) and of liver GR and phospho-Ser211 GR (right panel) in fast-refed and fast-fast samples, using actin as a loading control. (**C**) Mice (5 mice/group) were subject to 3 h or 16 h fasting, followed by i.p. injection with either solvent or with Dex (2 mg/kg) and GW (2 mg/kg) for 4 h. After sacrifice, livers were collected, snap-frozen and further processed for mRNA analysis via qPCR. Household genes were selected via GENORM (qBase software package) and relative expression levels were calculated. Data were analyzed for statistical significance using a non-parametric Wilcoxon rank sum test; * and ** denote *P*-values < 0.05 and < 0.01, respectively.

cooperative responses at the gene expression level can be pushed further when exogenously administering synthetic GR and PPARα ligands over a background of (catabolic) fasting, we compared groups of mice fasted for either 3 h or 16 h, after which Dex (2 mg/kg) and GW (2 mg/kg) was given i.p. for 4 h. qPCR results show that mRNA levels of *Pdk4* and *Ehhadh* are enhanced comparing 3 h versus 16 h fasting (Figure 7C). Administering a combination of Dex and GW to mice increases liver mRNA levels of these, and other, PPAR/GR controlled genes even further (Figure 7C and Supplementary Figure S9).

DISCUSSION

Nuclear receptor cross-talk is a fairly novel research area with potential therapeutic implications, as the behavior of two drug targets co-triggered may yield a different biological outcome compared to the single treatments. Cross-talk mechanisms offer an advantage to the organism, especially when exceptional conditions require a flexible adaptation of a particular gene repertoire. We report here on a novel nuclear receptor cross-talk mechanism in primary hepatocytes and in murine liver *in vivo*, emerging only under the specific condition of a prolonged starvation and aimed at key controlling genes of glucose and lipid metabolism. More specifically, we identified pAMPK as a new component associated with lipid metabolic gene promoters, recruited in response to both combined GR and PPARα activation specifically under culturing conditions mimicking starvation (Figure 6). This finding was recapitulated upon prolonged starvation in animals, relying on an endogenous activation of these nuclear receptors, which is expected following nutrient deprivation stress (Figure 7).

Previous studies observed that FAs or synthetic PPARα-ligands combined with GCs can synergistically induce *Ehhadh*, *Acox1* and peroxisomal thiolase expression in primary hepatocytes, hepatoma cells or rat liver *in vivo* (46–48) yet the underlying mechanism remained unclear. Up-regulation of PPARα by ligand-activated GR was proposed to explain this synergy and PPARα expression was shown to follow endogenous corticosterone levels in rats (49). While our own results in hepatocytes do support the up-regulation of PPARα by GCs (data not shown), this mechanism appears only part of the observed cross-talk. Indeed, by mapping GR and PPARα cistromes in primary hepatocytes, genomic binding sites of GR overlap more than half of the

PPARα cistrome (Figure 1). The functional significance of binding site co-localization is further supported by a strong enrichment of co-occupied regions in the vicinity of cooperatively co-regulated genes (Figure 3), supporting a role for a direct transcriptional regulation. Mechanistically, we found that the dependency of GR to co-localize with PPARα at PPRE genes occurs in a target gene-specific manner (Figure 2 and Supplementary Figure S2).

The regulation of the *Pdk4* gene (Figure 2), coding for an important control enzyme determining the fate of pyruvate, may either be consistent with a tethering recruitment model or else, may be explained by a role for PPARα as a chromatin-priming pioneering factor, as has been proposed for other transcription factors (50,51). Our data suggest that ligand-activated PPARα may facilitate or support GR recruitment to co-bound sites yet the presence of PPARα is clearly not an absolute pre-requisite for GR occupancy at other regulatory sites, e.g. as found for *Angptl4* (Figure 2). Nevertheless, the transcriptional activity of GR does depend on the presence of PPARα as Dex induction of co-regulated lipid metabolic genes was consistently reduced in PPARα-KO hepatocytes (Figure 5). The time-dependency of the cooperative gene induction (Figure 5) which is recapitulated following a fed-to-fast transition over longer times (Supplementary Figure S7A) correlates with a need for novel protein synthesis (Supplementary Figure S7B). This observation could theoretically be reconciled with a GC-induced increase of PPARα (49), as we found to be the case in hepatocytes (data not shown) or of levels of AMPK (52), or both. Surprisingly, we did not find mRNA upregulation of any of these genes in the liver samples following treatment of mice with Dex and GW after a prolonged fasting state (Supplementary Figure S10); a situation for which cooperativity on GR/PPARα co-controlled genes was apparent as depicted in Figure 7C. From our data, increased levels of yet another regulatory protein, possibly along with sustained proper modifications, i.e. phosphorylation of AMPK and GRα, may act in concert to build a protein complex able to mount a powerful fasting response at gene regulatory sites.

To explore additional levels of the cross-talk, we studied hepatocyte metabolite behavior following combined GR/PPARα activation. The results of the metabolomics experiment in primary hepatocytes showed that Dex treatment leads to the accumulation of intracellular FAs (Figure 4), in line with previous studies (Jia *et al.*, 2009) (53). Interestingly, the combined stimulation with a PPARα-agonist counteracted the lipogenic action of Dex and reversed FA levels back to the control condition. This result demonstrates that the intra-hepatic cross-talk between GR and PPARα exists also at the metabolite level, with the cooperative transcriptional response as a likely contributor to the observed reduction in FA levels.

The key mechanism of enzyme control behind the switch from FA oxidation to glucose utilization and lipogenesis upon fast-to-fed involves insulin-induced acetyl-CoA-carboxylase (ACC) activity (54). ACC catalyzes the first step of FA synthesis and produces malonyl–CoA, which acts as a potent allosteric inhibitor of Cpt1a, thus limiting mitochondrial FA import and oxidation (54–56). This process is reversed by AMPK during fasting, via AMPK-mediated phosphorylation and potent inhibition of ACC activity (57–59). While ACC inhibition by AMPK is a well-recognized mechanism, several studies indicate the importance of nuclear AMPK and its effects on gene expression. Indeed, AMPK was shown to phosphorylate and control the activity of several metabolic cofactors and transcription factors, including PGC1α (60), Med1 (61), CREB (62) and Foxo3 (63). The presence of both AMPKα1 and AMPKα2 subunits has been detected in the nucleus and was shown to be dynamically regulated (64–66) yet chromatin associations were thus far never reported. In line with our findings, nuclear translocation of the liver AMPKα1 catalytic subunit has been reported to follow circadian rhythms *in vivo* and to respond to low glucose conditions (66).

PPARα-ligands have also been demonstrated to increase both the phosphorylation and activity of AMPK (67,68). Although a direct interaction between PPARα and AMPK was observed before (69), the influence of AMPK activation on PPARα activity is still not completely clear. AMPK was shown to co-activate PPARα in an inactive ATP-bound state (69,70) but the effects of pharmacological AMPK activation on PPARα activity are contradictory, showing both inhibition (69,70) and activation (71). Similarly, GCs can activate liver AMPK (52) and pharmacological AMPK activation was shown to alter the effects of glucocorticoids on liver carbohydrate metabolism (13), however, via an indirect mechanism, involving p38 MAPK activation. In support of the findings of Nader *et al.*, we observe in murine liver, under conditions in which AMPK is expected to be active, i.e. prolonged fasting, that this indeed coincides with phosphorylation of GR at Ser211. We go on to show that refeeding dampens these modifications (Figure 7). Given the observation that PPARα, GR and pAMPK can form a trimeric complex *in vitro* (Figure 6), we postulate that AMPK may influence single GR or PPARα signaling pathways in a different manner as compared to a coordinately regulated cross-talk upon simultaneous co-signaling of GR and PPAR. Only the latter event seems to involve a direct chromatin recruitment of AMPK. Indeed, in line with our finding that phosphorylated AMPK is primarily retrieved at the promoters of GR/PPARα co-controlled genes, we show that AMPK inhibition is a strong cue to short circuit GC and PPARα agonist co-controlled cooperative gene expression of lipid catabolic genes (Figure 6). Importantly, the promoter recruitment of pAMPK was strongly enhanced upon combined activation of both nuclear receptors and this occurred only 5 h after cells underwent transition from a high-insulin, high glucose (fed) condition to a fasting state (Figure 6). This delayed recruitment of pAMPK was accompanied by an increase in transcriptional activity as measured by pPol2-Ser2 enrichment and associated with a regulatory switch from Dex-mediated repression to co-activation of *Pdk4* (Figure 6). An interaction between regulatory subunits of AMPK and PPARα but not GR, indicates that PPARα may be more likely to function as a direct physical contact point involved in the genomic pAMPK recruitment (Figure 6). Nevertheless, a GST-pull down experiment demonstrates that GRα can additionally associate, in support of the existence of a trimeric complex between these three proteins, albeit under *in vitro* conditions (Figure 6 and Supplementary Figure S8).

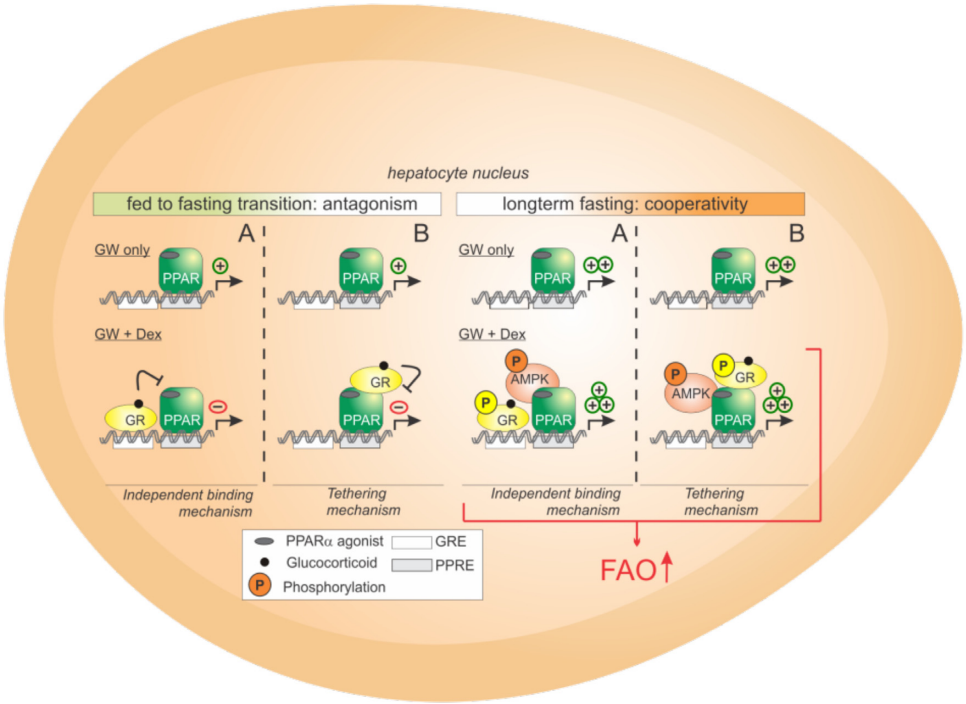

Figure 8. Chromatin recruitment of activated AMP kinase drives fasting response genes co-controlled by GR and PPARα. The model depicts concluding findings on transcriptional mechanisms, specifically for the subset of GC and PPARα agonist co-controlled lipid-oxidative-genes that are subject to changes of the nutritional state and that demonstrate pAMPK recruitment upon longterm fasting. Under this particular condition, our data are further consistent with an involvement of GR, phosphorylated at Ser211. The top row shows the transcriptional activity of genes only triggered by GW7647 (GW alone) whereas the bottom row shows transcriptional activity of genes triggered by GW7647 and Dex. A and B refer to the underlying mechanisms that were identified, with *Ehhadh* and *Angptl4* exemplifying genes for which independent transcription (**A**) factor binding was found and *Pdk4* being the prototypical example of a (**B**) tethering binding. Note that actually also a third subset of co-controlled genes was identified, i.e. lipid metabolism genes that are not subject to a nutritional switching mechanism but move from low to high cooperativity when progressing to catabolic fasting (not depicted here). FAO – Fatty Acid Oxidation.

In summary, we show that GR and PPARα cooperatively activate a lipid catabolic gene program in primary hepatocytes via a novel mechanism involving direct promoter recruitment of activated AMPK and we present a possible model in Figure 8 on how our combined data could be interpreted. Although we could show formation of a trimeric complex *in vitro*, we bid for caution when translating to the *in vivo* situation, as a limitation of our data is that we were unable, due to technical reasons, to unambiguously prove via re-ChIP that these proteins are also able to directly form a trimeric complex *in vivo* at the promoter level. Given the dependency of the transcriptional response to Dex and GW on AMPK activity/recruitment, an attenuated ligand response in fed as compared to fasted conditions and a recapitulation of a stronger AMPK chromatin recruitment in fasted as compared to refed mice along with confirmatory results *in vivo* that Dex/GW cooperatively triggers glucose/lipid metabolism genes in fasted liver (Figure 7), the observed cooperativity is likely most relevant for an adaptation of intra-hepatic metabolism to states of prolonged fasting, under which FAs serve as the main energy source.

SUPPLEMENTARY DATA

Supplementary Data are available at NAR Online.

ACKNOWLEDGEMENT

The authors thank Dr Stéphane Plaisance from the VIB Bio Informatics Training and Service Facility (VIB-BITS) for useful discussions and tutorials, Dieter Defever and Anne-Sophie De Smet (Receptor Research Laboratories, VIB) for the technical assistance with MAPPIT experiments and Dr Anje Cauwels for help with hepatocyte isolations.

FUNDING

Instituut voor Wetenschappelijk Technologisch onderzoek (IWT) Strategisch Basis Onderzoek (SBO-IWT) [100013 to C.L, J. T and K.D.B.]; European Research Council (ERC) Advanced Grant [N340941 to J.T.]; Fonds voor Wetenschappelijk Onderzoek (FWO)-Vlaanderen [G018013N to K.D.B]; Instituut voor Wetenschappelijk Technologisch onderzoek (IWT) Graduate Student Fellowship [093313 to D.R]; Interuniversity Attraction Poles (IAP) Programme of the Belgian Science Policy [P7/13 to J.T., K.D.B and M.H.R.]; UGent BOF (Bijzonder Onderzoeksfonds) Graduate Student Fellowship [to V.M]. Institut Universitaire de France (to B.S.). Funding for open access charge: BOF UGent [B/13453/01].

Conflict of interest statement. None declared.

REFERENCES

1. Braissant,O., Foufelle,F., Scotto,C., Dauca,M. and Wahli,W. (1996) Differential expression of peroxisome proliferator-activated receptors (PPARs): tissue distribution of PPAR-alpha, -beta, and -gamma in the adult rat. *Endocrinology*, **137**, 354–366.
2. Kersten,S., Seydoux,J., Peters,J.M., Gonzalez,F.J., Desvergne,B. and Wahli,W. (1999) Peroxisome proliferator-activated receptor alpha mediates the adaptive response to fasting. *J. Clin. Invest.*, **103**, 1489–1498.
3. Leone,T.C., Weinheimer,C.J. and Kelly,D.P. (1999) A critical role for the peroxisome proliferator-activated receptor alpha (PPARalpha) in the cellular fasting response: the PPARalpha-null mouse as a model of fatty acid oxidation disorders. *Proc. Natl. Acad. Sci. U. S. A.*, **96**, 7473–7478.
4. Rakhshandehroo,M., Knoch,B., Muller,M. and Kersten,S. (2010) Peroxisome proliferator-activated receptor alpha target genes. *PPAR Res.*, **2010**, 612089.
5. Delerive,P., De Bosscher,K., Besnard,S., Vanden Berghe,W., Peters,J.M., Gonzalez,F.J., Fruchart,J.C., Tedgui,A., Haegeman,G. and Staels,B. (1999) Peroxisome proliferator-activated receptor alpha negatively regulates the vascular inflammatory gene response by negative cross-talk with transcription factors NF-kappaB and AP-1. *J. Biol. Chem.*, **274**, 32048–32054.
6. Pawlak,M., Baugé,E., Bourguet,W., De Bosscher,K., Lalloyer,F., Tailleux,A., Lebherz,C., Lefebvre,P. and Staels,B. (2014) The transrepressive activity of peroxisome proliferator-activated receptor alpha is necessary and sufficient to prevent liver fibrosis in mice. *Hepatology*, **60**, 1593–1606.
7. Ratman,D., Vanden Berghe,W., Dejager,L., Libert,C., Tavernier,J., Beck,I.M. and De Bosscher,K. (2012) How glucocorticoid receptors modulate the activity of other transcription factors: A scope beyond tethering. *Mol. Cell. Endocrinol.*, **380**, 41–54.
8. Lim,H.-W., Uhlenhaut,N.H., Rauch,A., Weiner,J., Hübner,S., Hübner,N., Won,K.-J., Lazar,M.A., Tuckermann,J. and Steger,D.J. (2015) Genomic redistribution of GR monomers and dimers mediates transcriptional response to exogenous glucocorticoid in vivo. *Genome Res.*, **25**, 836–844.
9. Schiller,B.J., Chodankar,R., Watson,L.C., Stallcup,M.R. and Yamamoto,K.R. (2014) Glucocorticoid receptor binds half sites as a monomer and regulates specific target genes. *Genome Biol.*, **15**, 418.
10. De Bosscher,K., Vanden Berghe,W. and Haegeman,G. (2003) The interplay between the glucocorticoid receptor and nuclear factor-kappaB or activator protein-1: molecular mechanisms for gene repression. *Endocr. Rev.*, **24**, 488–522.
11. Bolli,G.B. and Fanelli,C.G. (1999) Physiology of glucose counterregulation to hypoglycemia. *Endocrinol. Metab. Clin. North Am.*, **28**, 467–493.
12. Hardie,D.G., Ross,F.A. and Hawley,S.A. (2012) AMPK: A nutrient and energy sensor that maintains energy homeostasis. *Nat. Rev. Mol. Cell Biol.*, **13**, 251–262.
13. Nader,N., Ng,S.S.M., Lambrou,G.I., Pervanidou,P., Wang,Y., Chrousos,G.P. and Kino,T. (2010) AMPK regulates metabolic actions of glucocorticoids by phosphorylating the glucocorticoid receptor through p38 MAPK. *Mol. Endocrinol.*, **24**, 1748–1764.
14. Bougarne,N., Paumelle,R., Caron,S., Hennuyer,N., Mansouri,R., Gervois,P., Staels,B., Haegeman,G. and De Bosscher,K. (2009) PPARalpha blocks glucocorticoid receptor alpha-mediated transactivation but cooperates with the activated glucocorticoid receptor alpha for transrepression on NF-kappaB. *Proc. Natl. Acad. Sci. U.S.A.*, **106**, 7397–7402.
15. Berry,M.N. and Friend,D.S. (1969) High-yield preparation of isolated rat liver parenchymal cells: A biochemical and fine structural study. *J. Cell Biol.*, **43**, 506–520.
16. Mokry,M., Hatzis,P., de Bruijn,E., Koster,J., Versteeg,R., Schuijers,J., van de Wetering,M., Guryev,V., Clevers,H. and Cuppen,E. (2010) Efficient double fragmentation ChIP-seq provides nucleotide resolution protein-DNA binding profiles. *PLoS One*, **5**, e15092.
17. Zhang,Y., Liu,T., Meyer,C.A., Eeckhoute,J., Johnson,D.S., Bernstein,B.E., Nusbaum,C., Myers,R.M., Brown,M., Li,W. *et al.* (2008) Model-based analysis of ChIP-Seq (MACS). *Genome Biol.*, **9**, R137.
18. Bailey,T.L., Boden,M., Buske,F.A., Frith,M., Grant,C.E., Clementi,L., Ren,J., Li,W.W. and Noble,W.S. (2009) MEME SUITE: Tools for motif discovery and searching. *Nucleic Acids Res.*, **37**, W202–W208.
19. Heinz,S., Benner,C., Spann,N., Bertolino,E., Lin,Y.C., Laslo,P., Cheng,J.X., Murre,C., Singh,H. and Glass,C.K. (2010) Simple combinations of lineage-determining transcription factors prime cis-regulatory elements required for macrophage and B cell identities. *Mol. Cell*, **38**, 576–589.
20. Grant,C.E., Bailey,T.L. and Noble,W.S. (2011) FIMO: Scanning for occurrences of a given motif. *Bioinformatics*, **27**, 1017–1018.
21. Quinlan,A.R. and Hall,I.M. (2010) BEDTools: A flexible suite of utilities for comparing genomic features. *Bioinformatics*, **26**, 841–842.
22. Trapnell,C., Pachter,L. and Salzberg,S.L. (2009) TopHat: discovering splice junctions with RNA-Seq. *Bioinformatics*, **25**, 1105–1111.
23. Trapnell,C., Williams,B.A., Pertea,G., Mortazavi,A., Kwan,G., van Baren,M.J., Salzberg,S.L., Wold,B.J. and Pachter,L. (2010) Transcript assembly and quantification by RNA-Seq reveals unannotated transcripts and isoform switching during cell differentiation. *Nat. Biotechnol.*, **28**, 511–515.
24. Goff,L., Trapnell,C. and Kelley,D. (2012) cummeRbund: Analysis, exploration, manipulation, and visualization of Cufflinks high-throughput sequencing data.
25. Young,M.D., Wakefield,M.J., Smyth,G.K. and Oshlack,A. (2010) Gene ontology analysis for RNA-seq: accounting for selection bias. *Genome Biol.*, **11**, R14.
26. Hellemans,J., Mortier,G., De Paepe,A., Speleman,F. and Vandesompele,J. (2007) qBase relative quantification framework and software for management and automated analysis of real-time quantitative PCR data. *Genome Biol.*, **8**, R19.
27. Lievens,S., Vanderroost,N., Van der Heyden,J., Gesellchen,V., Vidal,M. and Tavernier,J. (2009) Array MAPPIT: High-throughput interactome analysis in mammalian cells. *J. Proteome Res.*, **8**, 877–886.
28. Beck,I.M., Drebert,Z.J., Hoya-Arias,R., Bahar,A.A., Devos,M., Clarisse,D., Desmet,S., Bougarne,N., Ruttens,B., Gossye,V. *et al.* (2013) Compound A, a selective glucocorticoid receptor modulator, enhances heat shock protein Hsp70 gene promoter activation. *PLoS One*, **8**, e69115.
29. Risseeuw,M.D.P., De Clercq,D.J.H., Lievens,S., Hillaert,U., Sinnaeve,D., Van den Broeck,F., Martins,J.C., Tavernier,J. and Van Calenbergh,S. (2013) A 'clickable' MTX reagent as a practical tool for profiling small-molecule-intracellular target interactions via MASPIT. *ChemMedChem*, **8**, 521–526.
30. Yang,X., Boehm,J.S., Yang,X., Salehi-Ashtiani,K., Hao,T., Shen,Y., Lubonja,R., Thomas,S.R., Alkan,O., Bhimdi,T. *et al.* (2011) A public genome-scale lentiviral expression library of human ORFs. *Nat. Methods*, **8**, 659–661.
31. Liu,T., Ortiz,J.A., Taing,L., Meyer,C.A., Lee,B., Zhang,Y., Shin,H., Wong,S.S., Ma,J., Lei,Y. *et al.* (2011) Cistrome: An integrative platform for transcriptional regulation studies. *Genome Biol.*, **12**, R83.
32. Lee,S.S. and Gonzalez,F.J. (1996) Targeted disruption of the peroxisome proliferator-activated receptor alpha gene, PPAR alpha. *Ann. N. Y. Acad. Sci.*, **804**, 524–529.
33. Koliwad,S.K., Gray,N.E. and Wang,J.C. (2012) Angiopoietin-like 4 (Angptl4): A glucocorticoid-dependent gatekeeper of fatty acid flux during fasting. *Adipocyte*, **1**, 182–187.
34. Rufer,A.C., Thoma,R., Benz,J., Stihle,M., Gsell,B., De Roo,E., Banner,D.W., Mueller,F., Chomienne,O. and Hennig,M. (2006) The crystal structure of carnitine palmitoyltransferase 2 and implications for diabetes treatment. *Structure*, **14**, 713–723.
35. Sebastian,D., Guitart,M., Garcia-Martinez,C., Mauvezin,C., Orellana-Gavalda,J.M., Serra,D., Gomez-Foix,A.M., Hegardt,F.G. and Asins,G. (2009) Novel role of FATP1 in mitochondrial fatty acid oxidation in skeletal muscle cells. *J. Lipid Res.*, **50**, 1789–1799.
36. Veerkamp,J.H., Van Moerkerk,H.T. and Zimmerman,A.W. (2000) Effect of fatty acid-binding proteins on intermembrane fatty acid transport studies on different types and mutant proteins. *Eur. J. Biochem.*, **267**, 5959–5966.
37. Huhtinen,K., O'Byrne,J., Lindquist,P.J., Contreras,J.A. and Alexson,S.E. (2002) The peroxisome proliferator-induced cytosolic type I acyl-CoA thioesterase (CTE-I) is a serine-histidine-aspartic acid alpha /beta hydrolase. *J. Biol. Chem.*, **277**, 3424–3432.

38. Hunt,M.C., Rautanen,A., Westin,M.A., Svensson,L.T. and Alexson,S.E. (2006) Analysis of the mouse and human acyl-CoA thioesterase (ACOT) gene clusters shows that convergent, functional evolution results in a reduced number of human peroxisomal ACOTs. *FASEB J.*, **20**, 1855–1864.
39. Radner,F.P., Streith,I.E., Schoiswohl,G., Schweiger,M., Kumari,M., Eichmann,T.O., Rechberger,G., Koefeler,H.C., Eder,S., Schauer,S. *et al.* (2010) Growth retardation, impaired triacylglycerol catabolism, hepatic steatosis, and lethal skin barrier defect in mice lacking comparative gene identification-58 (CGI-58). *J. Biol. Chem.*, **285**, 7300–7311.
40. Boukaftane,Y., Duncan,A., Wang,S., Labuda,D., Robert,M.F., Sarrazin,J., Schappert,K. and Mitchell,G.A. (1994) Human mitochondrial HMG CoA synthase: liver cDNA and partial genomic cloning, chromosome mapping to 1p12-p13, and possible role in vertebrate evolution. *Genomics*, **23**, 552–559.
41. Ning,J., Xi,G. and Clemmons,D.R. (2011) Suppression of AMPK activation via S485 phosphorylation by IGF-I during hyperglycemia is mediated by AKT activation in vascular smooth muscle cells. *Endocrinology*, **152**, 3143–3154.
42. Valentine,R.J., Coughlan,K.A., Ruderman,N.B. and Saha,A.K. (2014) Insulin inhibits AMPK activity and phosphorylates AMPK Ser485/491 through Akt in hepatocytes, myotubes and incubated rat skeletal muscle. *Arch. Biochem. Biophys.*, **562**, 62–69.
43. Eyckerman,S., Verhee,A., der Heyden,J.V., Lemmens,I., Ostade,X.V., Vandekerckhove,J. and Tavernier,J. (2001) Design and application of a cytokine-receptor-based interaction trap. *Nat. Cell Biol.*, **3**, 1114–1119.
44. Bultot,L., Guigas,B., Von Wilamowitz-Moellendorff,A., Maisin,L., Vertommen,D., Hussain,N., Beullens,M., Guinovart,J.J., Foretz,M., Viollet,B. *et al.* (2012) AMP-activated protein kinase phosphorylates and inactivates liver glycogen synthase. *Biochem. J.*, **443**, 193–203.
45. Ismaili,N. and Garabedian,M.J. (2004) Modulation of glucocorticoid receptor function via phosphorylation. *Ann. N. Y. Acad. Sci.*, **1024**, 86–101.
46. Lemberger,T., Staels,B., Saladin,R., Desvergne,B., Auwerx,J. and Wahli,W. (1994) Regulation of the peroxisome proliferator-activated receptor alpha gene by glucocorticoids. *J. Biol. Chem.*, **269**, 24527–24530.
47. Sorensen,H.N., Gautik,K.M., Bremer,J. and Spydevold,O. (1992) Induction of the three peroxisomal β-oxidation enzymes is synergistically regulated by dexamethasone and fatty acids, and counteracted by insulin in Morris 7800C1 hepatoma cells in culture. *Eur. J. Biochem.*, **208**, 705–711.
48. Steineger,H.H., Sorensen,H.N., Tugwood,J.D., Skrede,S., Spydevold,O. and Gautvik,K.M. (1994) Dexamethasone and insulin demonstrate marked and opposite regulation of the steady-state mRNA level of the peroxisomal proliferator-activated receptor (PPAR) in hepatic cells. Hormonal modulation of fatty-acid-induced transcription. *Eur. J. Biochem.*, **225**, 967–974.
49. Lemberger,T., Saladin,R., Vázquez,M., Assimacopoulos,F., Staels,B., Desvergne,B., Wahli,W. and Auwerx,J. (1996) Expression of the Peroxisome Proliferator-activated Receptor Gene Is Stimulated by Stress and Follows a Diurnal Rhythm. *J. Biol. Chem.*, **271**, 1764–1769.
50. Siersbæk,R., Nielsen,R., John,S., Sung,M.-H., Baek,S., Loft,A., Hager,G.L. and Mandrup,S. (2011) Extensive chromatin remodelling and establishment of transcription factor 'hotspots' during early adipogenesis. *EMBO J.*, **30**, 1459–1472.
51. Cardamone,M.D., Tanasa,B., Chan,M., Cederquist,C.T., Andricovich,J., Rosenfeld,M.G., Perissi,V., Ahmadian,M., Duncan,R.E., Varady,K.A. *et al.* (2014) GPS2/KDM4A pioneering activity regulates promoter-specific recruitment of PPARγ. *Cell Rep.*, **8**, 163–176.
52. Christ-Crain,M., Kola,B., Lolli,F., Fekete,C., Seboek,D., Wittmann,G., Feltrin,D., Igreja,S.C., Ajodha,S., Harvey-White,J. *et al.* (2008) AMP-activated protein kinase mediates glucocorticoid-induced metabolic changes: a novel mechanism in Cushing's syndrome. *FASEB J.*, **22**, 1672–1683.
53. Letteron,P., Brahimi-Bourouina,N., Robin,M.A., Moreau,A., Feldmann,G. and Pessayre,D. (1997) Glucocorticoids inhibit mitochondrial matrix acyl-CoA dehydrogenases and fatty acid beta-oxidation. *Am. J. Physiol.*, **272**, G1141–G1150.
54. Abu-Elheiga,L., Matzuk,M.M., Abo-Hashema,K.A. and Wakil,S.J. (2001) Continuous fatty acid oxidation and reduced fat storage in mice lacking acetyl-CoA carboxylase 2. *Science*, **291**, 2613–2616.
55. McGarry,J.D., Mannaerts,G.P. and Foster,D.W. (1977) A possible role for malonyl-CoA in the regulation of hepatic fatty acid oxidation and ketogenesis. *J. Clin. Invest.*, **60**, 265–270.
56. McGarry,J.D. and Brown,N.F. (1997) The mitochondrial carnitine palmitoyltransferase system. From concept to molecular analysis. *Eur. J. Biochem.*, **244**, 1–14.
57. Dyck,J.R., Kudo,N., Barr,A.J., Davies,S.P., Hardie,D.G. and Lopaschuk,G.D. (1999) Phosphorylation control of cardiac acetyl-CoA carboxylase by cAMP-dependent protein kinase and 5′-AMP activated protein kinase. *Eur. J. Biochem.*, **262**, 184–190.
58. Munday,M.R., Campbell,D.G., Carling,D. and Hardie,D.G. (1988) Identification by amino acid sequencing of three major regulatory phosphorylation sites on rat acetyl-CoA carboxylase. *Eur. J. Biochem.*, **175**, 331–338.
59. O'Neill,H.M., Lally,J.S., Galic,S., Thomas,M., Azizi,P.D., Fullerton,M.D., Smith,B.K., Pulinilkunnil,T., Chen,Z., Samaan,M.C. *et al.* (2014) AMPK phosphorylation of ACC2 is required for skeletal muscle fatty acid oxidation and insulin sensitivity in mice. *Diabetologia*, **57**, 1693–1702.
60. Jäger,S., Handschin,C., St-Pierre,J. and Spiegelman,B.M. (2007) AMP-activated protein kinase (AMPK) action in skeletal muscle via direct phosphorylation of PGC-1alpha. *Proc. Natl. Acad. Sci. U.S.A.*, **104**, 12017–12022.
61. Viswakarma,N., Jia,Y., Bai,L., Gao,Q., Lin,B., Zhang,X., Misra,P., Rana,A., Jain,S., Gonzalez,F.J. *et al.* (2013) The Med1 subunit of the mediator complex induces liver cell proliferation and is phosphorylated by AMP kinase. *J. Biol. Chem.*, **288**, 27898–27911.
62. Thomson,D.M., Herway,S.T., Fillmore,N., Kim,H., Brown,J.D., Barrow,J.R. and Winder,W.W. (2007) AMP-activated protein kinase phosphorylates transcription factors of the CREB family. *J. Appl. Physiol.*, **104**, 429–438.
63. Greer,E.L., Oskoui,P.R., Banko,M.R., Maniar,J.M., Gygi,M.P., Gygi,S.P. and Brunet,A. (2007) The energy sensor AMP-activated protein kinase directly regulates the mammalian FOXO3 transcription factor. *J. Biol. Chem.*, **282**, 30107–30119.
64. Salt,I., Celler,J.W., Hawley,S.A., Prescott,A., Woods,A., Carling,D. and Hardie,D.G. (1998) AMP-activated protein kinase: greater AMP dependence, and preferential nuclear localization, of complexes containing the alpha2 isoform. *Biochem. J.*, **334**, 177–187.
65. Suzuki,A., Okamoto,S., Lee,S., Saito,K., Shiuchi,T. and Minokoshi,Y. (2007) Leptin stimulates fatty acid oxidation and peroxisome proliferator-activated receptor alpha gene expression in mouse C2C12 myoblasts by changing the subcellular localization of the alpha2 form of AMP-activated protein kinase. *Mol. Cell. Biol.*, **27**, 4317–4327.
66. Lamia,K.A., Sachdeva,U.M., DiTacchio,L., Williams,E.C., Alvarez,J.G., Egan,D.F., Vasquez,D.S., Juguilon,H., Panda,S., Shaw,R.J. *et al.* (2009) AMPK regulates the circadian clock by cryptochrome phosphorylation and degradation. *Science*, **326**, 437–440.
67. Liangpunsakul,S., Wou,S.-E., Wineinger,K.D., Zeng,Y., Cyganek,I., Jayaram,H.N. and Crabb,D.W. (2009) Effects of WY-14, 643 on the phosphorylation and activation of AMP-dependent protein kinase. *Arch. Biochem. Biophys.*, **485**, 10–15.
68. Okayasu,T., Tomizawa,A., Suzuki,K., Manaka,K. and Hattori,Y. (2008) PPARalpha activators upregulate eNOS activity and inhibit cytokine-induced NF-kappaB activation through AMP-activated protein kinase activation. *Life Sci.*, **82**, 884–891.
69. Bronner,M., Hertz,R. and Bar-Tana,J. (2004) Kinase-independent transcriptional co-activation of peroxisome proliferator-activated receptor alpha by AMP-activated protein kinase. *Biochem. J.*, **384**, 295–305.
70. Sozio,M.S., Lu,C., Zeng,Y., Liangpunsakul,S. and Crabb,D.W. (2011) Activated AMPK inhibits PPAR-{alpha} and PPAR-{gamma} transcriptional activity in hepatoma cells. *Am. J. Physiol. Gastrointest. Liver Physiol.*, **301**, G739–G747.
71. Houten,S.M., Chegary,M., Te Brinke,H., Wijnen,W.J., Glatz,J.F.C., Luiken,J.J.F.P., Wijburg,F.A. and Wanders,R.J.A. (2009) Pyruvate dehydrogenase kinase 4 expression is synergistically induced by AMP-activated protein kinase and fatty acids. *Cell. Mol. Life Sci.*, **66**, 1283–1294.